Scaling violations and determination of α_s from jet production in γp interactions at HERA

ZEUS Collaboration

S. Chekanov, D. Krakauer, J.H. Loizides [1], S. Magill, B. Musgrave, J. Repond, R. Yoshida

Argonne National Laboratory, Argonne, IL 60439-4815, USA [49]

M.C.K. Mattingly

Andrews University, Berrien Springs, MI 49104-0380, USA

P. Antonioli, G. Bari, M. Basile, L. Bellagamba, D. Boscherini, A. Bruni, G. Bruni, G. Cara Romeo, L. Cifarelli, F. Cindolo, A. Contin, M. Corradi, S. De Pasquale, P. Giusti, G. Iacobucci, A. Margotti, R. Nania, F. Palmonari, A. Pesci, G. Sartorelli, A. Zichichi

University and INFN Bologna, Bologna, Italy [40]

G. Aghuzumtsyan, D. Bartsch, I. Brock, S. Goers, H. Hartmann, E. Hilger, P. Irrgang, H.-P. Jakob, A. Kappes [2], U.F. Katz [2], O. Kind, E. Paul, J. Rautenberg [3], R. Renner, H. Schnurbusch, A. Stifutkin, J. Tandler, K.C. Voss, M. Wang, A. Weber

Physikalisches Institut der Universität Bonn, Bonn, Germany [37]

D.S. Bailey [4], N.H. Brook [4], J.E. Cole, B. Foster, G.P. Heath, H.F. Heath, S. Robins, E. Rodrigues [5], J. Scott, R.J. Tapper, M. Wing

H.H. Wills Physics Laboratory, University of Bristol, Bristol, United Kingdom [48]

M. Capua, A. Mastroberardino, M. Schioppa, G. Susinno

Calabria University, Physics Department and INFN, Cosenza, Italy [40]

J.Y. Kim, Y.K. Kim, J.H. Lee, I.T. Lim, M.Y. Pac [6]

Chonnam National University, Kwangju, South Korea [42]

A. Caldwell [7], M. Helbich, X. Liu, B. Mellado, Y. Ning, S. Paganis, Z. Ren,
W.B. Schmidke, F. Sciulli

Nevis Laboratories, Columbia University, Irvington on Hudson, NY 10027, USA [50]

J. Chwastowski, A. Eskreys, J. Figiel, K. Olkiewicz, P. Stopa, L. Zawiejski

Institute of Nuclear Physics, Cracow, Poland [44]

L. Adamczyk, T. Bołd, I. Grabowska-Bołd, D. Kisielewska, A.M. Kowal, M. Kowal,
T. Kowalski, M. Przybycień, L. Suszycki, D. Szuba, J. Szuba [8]

Faculty of Physics and Nuclear Techniques, University of Mining and Metallurgy, Cracow, Poland [51]

A. Kotański [9], W. Słomiński [10]

Department of Physics, Jagellonian University, Cracow, Poland

L.A.T. Bauerdick [11], U. Behrens, I. Bloch, K. Borras, V. Chiochia, D. Dannheim,
M. Derrick [12], G. Drews, J. Fourletova, A. Fox-Murphy [13], U. Fricke, A. Geiser,
F. Goebel [7], P. Göttlicher [14], O. Gutsche, T. Haas, W. Hain, G.F. Hartner, S. Hillert,
U. Kötz, H. Kowalski [15], G. Kramberger, H. Labes, D. Lelas, B. Löhr, R. Mankel,
I.-A. Melzer-Pellmann, M. Moritz [16], D. Notz, M.C. Petrucci [17], A. Polini, A. Raval,
U. Schneekloth, F. Selonke [18], H. Wessoleck, R. Wichmann [19], G. Wolf, C. Youngman,
W. Zeuner

Deutsches Elektronen-Synchrotron DESY, Hamburg, Germany

A. Lopez-Duran Viani [20], A. Meyer, S. Schlenstedt

DESY Zeuthen, Zeuthen, Germany

G. Barbagli, E. Gallo, C. Genta, P.G. Pelfer

University and INFN, Florence, Italy [40]

A. Bamberger, A. Benen, N. Coppola

Fakultät für Physik der Universität Freiburg i.Br., Freiburg i.Br., Germany [37]

M. Bell, P.J. Bussey, A.T. Doyle, C. Glasman, J. Hamilton, S. Hanlon, S.W. Lee,
A. Lupi, D.H. Saxon, I.O. Skillicorn

Department of Physics and Astronomy, University of Glasgow, Glasgow, United Kingdom [48]

I. Gialas

Department of Engineering in Management and Finance, University of Aegean, Greece

B. Bodmann, T. Carli, U. Holm, K. Klimek, N. Krumnack, E. Lohrmann, M. Milite, H. Salehi, S. Stonjek [21], K. Wick, A. Ziegler, Ar. Ziegler

Hamburg University, Institute of Experimental Physics, Hamburg, Germany [37]

C. Collins-Tooth, C. Foudas, R. Gonçalo [5], K.R. Long, F. Metlica, A.D. Tapper

Imperial College London, High Energy Nuclear Physics Group, London, United Kingdom [48]

P. Cloth, D. Filges

Forschungszentrum Jülich, Institut für Kernphysik, Jülich, Germany

M. Kuze, K. Nagano, K. Tokushuku [22], S. Yamada, Y. Yamazaki

Institute of Particle and Nuclear Studies, KEK, Tsukuba, Japan [41]

A.N. Barakbaev, E.G. Boos, N.S. Pokrovskiy, B.O. Zhautykov

Institute of Physics and Technology of Ministry of Education and Science of Kazakhstan, Almaty, Kazakhstan

H. Lim, D. Son

Kyungpook National University, Taegu, South Korea [42]

F. Barreiro, O. González, L. Labarga, J. del Peso, I. Redondo [23], E. Tassi, J. Terrón, M. Vázquez

Departamento de Física Teórica, Universidad Autónoma de Madrid, Madrid, Spain [47]

M. Barbi, A. Bertolin, F. Corriveau, S. Gliga, J. Lainesse, S. Padhi, D.G. Stairs

Department of Physics, McGill University, Montréal, Québec, H3A 2T8 Canada [36]

T. Tsurugai

Meiji Gakuin University, Faculty of General Education, Yokohama, Japan

A. Antonov, P. Danilov, B.A. Dolgoshein, D. Gladkov, V. Sosnovtsev, S. Suchkov

Moscow Engineering Physics Institute, Moscow, Russia [45]

R.K. Dementiev, P.F. Ermolov, Yu.A. Golubkov, I.I. Katkov, L.A. Khein, I.A. Korzhavina, V.A. Kuzmin, B.B. Levchenko, O.Yu. Lukina, A.S. Proskuryakov,

L.M. Shcheglova, N.N. Vlasov, S.A. Zotkin

Moscow State University, Institute of Nuclear Physics, Moscow, Russia [46]

C. Bokel, J. Engelen, S. Grijpink, E. Koffeman, P. Kooijman, E. Maddox, A. Pellegrino,
S. Schagen, H. Tiecke, N. Tuning, J.J. Velthuis, L. Wiggers, E. de Wolf

NIKHEF and University of Amsterdam, Amsterdam, Netherlands [43]

N. Brümmer, B. Bylsma, L.S. Durkin, T.Y. Ling

Physics Department, Ohio State University, Columbus, OH 43210, USA [49]

S. Boogert, A.M. Cooper-Sarkar, R.C.E. Devenish, J. Ferrando, G. Grzelak,
T. Matsushita, M. Rigby, O. Ruske [24], M.R. Sutton, R. Walczak

Department of Physics, University of Oxford, Oxford, United Kingdom [48]

R. Brugnera, R. Carlin, F. Dal Corso, S. Dusini, A. Garfagnini, S. Limentani,
A. Longhin, A. Parenti, M. Posocco, L. Stanco, M. Turcato

Dipartimento di Fisica dell' Università and INFN, Padova, Italy [40]

E.A. Heaphy, B.Y. Oh, P.R.B. Saull [25], J.J. Whitmore [26]

Department of Physics, Pennsylvania State University, University Park, PA 16802, USA [50]

Y. Iga

Polytechnic University, Sagamihara, Japan [41]

G. D'Agostini, G. Marini, A. Nigro

Dipartimento di Fisica, Università 'La Sapienza' and INFN, Rome, Italy [40]

C. Cormack [27], J.C. Hart, N.A. McCubbin

Rutherford Appleton Laboratory, Chilton, Didcot, Oxon, United Kingdom [48]

C. Heusch

University of California, Santa Cruz, CA 95064, USA [49]

I.H. Park

Department of Physics, Ewha Womans University, Seoul, South Korea

N. Pavel

Fachbereich Physik der Universität-Gesamthochschule Siegen, Germany

H. Abramowicz, A. Gabareen, S. Kananov, A. Kreisel, A. Levy

Raymond and Beverly Sackler Faculty of Exact Sciences, School of Physics, Tel Aviv University, Tel Aviv, Israel [39]

T. Abe, T. Fusayasu, S. Kagawa, T. Kohno, T. Tawara, T. Yamashita

Department of Physics, University of Tokyo, Tokyo, Japan [41]

R. Hamatsu, T. Hirose [18], M. Inuzuka, S. Kitamura [28], K. Matsuzawa, T. Nishimura

Tokyo Metropolitan University, Department of Physics, Tokyo, Japan [41]

M. Arneodo [29], M.I. Ferrero, V. Monaco, M. Ruspa, R. Sacchi, A. Solano

Università di Torino, Dipartimento di Fisica Sperimentale and INFN, Torino, Italy [40]

R. Galea, T. Koop, G.M. Levman, J.F. Martin, A. Mirea, A. Sabetfakhri

Department of Physics, University of Toronto, Toronto, Ontario, M5S 1A7 Canada [36]

J.M. Butterworth, C. Gwenlan, R. Hall-Wilton, T.W. Jones, M.S. Lightwood, B.J. West

Physics and Astronomy Department, University College London, London, United Kingdom [48]

J. Ciborowski [30], R. Ciesielski [31], R.J. Nowak, J.M. Pawlak, B. Smalska [32], J. Sztuk [33], T. Tymieniecka [34], A. Ukleja [34], J. Ukleja, A.F. Żarnecki

Warsaw University, Institute of Experimental Physics, Warsaw, Poland [52]

M. Adamus, P. Plucinski

Institute for Nuclear Studies, Warsaw, Poland [52]

Y. Eisenberg, L.K. Gladilin [35], D. Hochman, U. Karshon

Department of Particle Physics, Weizmann Institute, Rehovot, Israel [38]

D. Kçira, S. Lammers, L. Li, D.D. Reeder, A.A. Savin, W.H. Smith

Department of Physics, University of Wisconsin, Madison, WI 53706, USA [49]

A. Deshpande, S. Dhawan, V.W. Hughes, P.B. Straub

Department of Physics, Yale University, New Haven, CT 06520-8121, USA [49]

S. Bhadra, C.D. Catterall, S. Fourletov, S. Menary, M. Soares, J. Standage

Department of Physics, York University, Ontario, M3J 1P3 Canada [36]

Abstract

Differential cross sections for jet photoproduction in the reaction $ep \rightarrow e$ jet X have been measured with the ZEUS detector at HERA using 82.2 pb^{-1} of integrated luminosity. Inclusive jet cross sections are presented as a function of the jet transverse energy, E_T^{jet}, for jets with $E_T^{\text{jet}} > 17$ GeV and pseudorapidity $-1 < \eta^{\text{jet}} < 2.5$, in the γp centre-of-mass-energy range $142 < W_{\gamma p} < 293$ GeV. Scaled jet invariant cross sections are presented as a function of the dimensionless variable $x_T \equiv 2E_T^{\text{jet}}/W_{\gamma p}$ for $\langle W_{\gamma p} \rangle = 180$ and 255 GeV. Next-to-leading-order QCD calculations give a good description of the measured differential cross sections in both magnitude and shape. The ratio of scaled jet invariant cross sections at the two $\langle W_{\gamma p} \rangle$ values shows clear non-scaling behaviour. A value for the strong coupling constant of $\alpha_s(M_Z) = 0.1224 \pm 0.0001(\text{stat.})^{+0.0022}_{-0.0019}(\text{exp.})^{+0.0054}_{-0.0042}(\text{th.})$ has been extracted from a QCD analysis of the measured $d\sigma/dE_T^{\text{jet}}$. The variation of α_s with E_T^{jet} is in good agreement with the running of α_s as predicted by QCD.

1. Introduction

Jet production provides a testing ground for the theory of the strong interaction between quarks and gluons, namely quantum chromodynamics (QCD). This Letter concentrates on one aspect of jet production, namely, the comparison of jet cross sections for the same reaction at different centre-of-mass energies. This highlights the effects of scaling violations, while a QCD analysis of jet-production rates allows the measurement of the strong coupling constant, α_s.

The parton model predicts a jet cross section that scales with the centre-of-mass energy. In this case, the scaled jet invariant cross section,

$$\frac{(E_T^{\text{jet}})^4 E^{\text{jet}} d^3\sigma}{dp_X^{\text{jet}} dp_Y^{\text{jet}} dp_Z^{\text{jet}}},$$

as a function of the dimensionless variable $x_T \equiv 2E_T^{\text{jet}}/W$, should be independent of W, where W is the centre-of-mass energy, E^{jet} is the jet energy,

E_T^{jet} is the jet transverse energy and $(p_X^{\text{jet}}, p_Y^{\text{jet}}, p_Z^{\text{jet}})$ are the components of the jet momentum. Thus, the ratio of scaled jet invariant cross sections for different centre-of-mass energies will be unity for all x_T. On the other hand, QCD predicts that jet cross sections should exhibit a non-scaling behaviour, due both to the evolution of the structure functions of the colliding hadrons and to the running of α_s. Scaling violations have been observed in the ratio of the scaled jet invariant cross sections as a function of x_T in $p\bar{p}$ collisions at centre-of-mass energies of either 546 or 630 and 1800 GeV [1].

At HERA, similar tests can be made in the photoproduction of jets. Two types of QCD processes contribute to jet production in γp interactions at $\mathcal{O}(\alpha\alpha_s)$ [2,3]: either the photon interacts directly with a parton in the proton (the direct process) or the photon acts as a source of partons, one of which interacts with a parton in the proton (the resolved process). Violations of scaling should be observed both in resolved and direct processes. Furthermore, measurements of high-E_T^{jet} jet cross sections in γp interactions over a wide range of E_T^{jet} allow a determination of $\alpha_s(M_Z)$ as well as its energy-scale dependence.

This Letter presents a measurement of the inclusive jet cross section in γp interactions as a function of E_T^{jet} in the γp centre-of-mass-energy range $142 < W_{\gamma p} < 293$ GeV for jets with pseudorapidity $-1 < \eta^{\text{jet}} < 2.5$. Scaled jet invariant cross sections are also presented as a function of x_T for $\langle W_{\gamma p} \rangle = 180$ and 255 GeV in the region $-2 < \eta_{\gamma p}^{\text{jet}} < 0$, where $\eta_{\gamma p}^{\text{jet}}$ is the jet pseudorapidity in the γp centre-of-mass frame.

2. Experimental conditions

The data were collected during the running period 1998–2000, when HERA operated with protons of energy $E_p = 920$ GeV and electrons or positrons of energy $E_e = 27.5$ GeV, and correspond to an integrated luminosity of 82.2 ± 1.9 pb^{-1}. A detailed description of the ZEUS detector can be found elsewhere [4,5]. A brief outline of the components that are most relevant for this analysis is given below.

Charged particles are tracked in the central tracking detector (CTD) [6], which operates in a magnetic field of 1.43 T provided by a thin superconducting solenoid.

The CTD consists of 72 cylindrical drift-chamber layers, organized in nine superlayers covering the polar-angle[53] region $15° < \theta < 164°$. The transverse-momentum resolution for full-length tracks can be parameterized as $\sigma(p_T)/p_T = 0.0058 p_T \oplus 0.0065 \oplus 0.0014/p_T$, with p_T in GeV. The tracking system was used to measure the interaction vertex with a typical resolution along (transverse to) the beam direction of 0.4 (0.1) cm and to cross-check the energy scale of the calorimeter.

The high-resolution uranium-scintillator calorimeter (CAL) [7] covers 99.7% of the total solid angle and consists of three parts: the forward (FCAL), the barrel (BCAL) and the rear (RCAL) calorimeters. Each part is subdivided transversely into towers and longitudinally into one electromagnetic section (EMC) and either one (in RCAL) or two (in BCAL and FCAL) hadronic sections (HAC). The smallest subdivision of the calorimeter is called a cell. Under test-beam conditions, the CAL single-particle relative energy resolutions were $\sigma(E)/E = 0.18/\sqrt{E \text{ (GeV)}}$ for electrons and $\sigma(E)/E = 0.35/\sqrt{E \text{ (GeV)}}$ for hadrons.

The luminosity was measured from the rate of the bremsstrahlung process $e^+ p \to e^+ \gamma p$. The resulting small-angle energetic photons were measured by the luminosity monitor [8], a lead-scintillator calorimeter placed in the HERA tunnel at $Z = -107$ m.

3. Data selection and jet search

A three-level trigger system was used to select events online [5,9]. At the first level, events were triggered by a coincidence of a regional or transverse energy sum in the CAL and at least one track from the interaction point measured in the CTD. At the second level, a total transverse energy of at least 8 GeV, excluding the energy in the eight CAL towers immediately surrounding the forward beampipe, was required, and cuts on CAL energies and timing were used to suppress events caused by interactions between the proton beam and residual gas in the beampipe. At the

third level, a jet algorithm was applied to the CAL cells and jets were reconstructed using the energies and positions of these cells. Events with at least one jet with $E_T > 10$ GeV and $\eta < 2.5$ were accepted.

Events from collisions between quasi-real photons and protons were selected offline using similar criteria to those reported in a previous publication [10]. The main steps are briefly discussed here. After requiring a reconstructed event vertex consistent with the nominal interaction position and cuts based on the tracking information, the contamination from beam-gas interactions, cosmic-ray showers and beam-halo muons was negligible. Charged current deep inelastic scattering (DIS) events were rejected by requiring the total missing transverse momentum, p_T^{miss}, to be small compared to the total transverse energy, E_T^{tot}, i.e., $p_T^{\text{miss}}/\sqrt{E_T^{\text{tot}}} < 2\sqrt{\text{GeV}}$. Any neutral current (NC) DIS events with an identified scattered-positron or electron candidate in the CAL [11] were removed from the sample using the method described previously [12]. The remaining background from NC DIS events was estimated by Monte Carlo (MC) techniques to be below 0.3% and was neglected. The selected sample consisted of events from ep interactions with $Q^2 \lesssim 1$ GeV^2 and a median $Q^2 \approx 10^{-3}$ GeV^2, where Q^2 is the virtuality of the exchanged photon. The events were restricted to γp centre-of-mass energies in the range $142 < W_{\gamma p} < 293$ GeV, as described in Section 6.

The longitudinally-invariant k_T cluster algorithm [13] was used in the inclusive mode [14] to reconstruct jets in the hadronic final state from the energy deposits in the CAL cells. The jet search was performed in the pseudorapidity–azimuth (η–φ) plane of the laboratory frame. The jet variables were defined according to the Snowmass convention [15]. The jets reconstructed from the CAL cell energies are called calorimetric jets and the variables associated with them are denoted by $E_{T,\text{cal}}^{\text{jet}}$, $\eta_{\text{cal}}^{\text{jet}}$ and $\varphi_{\text{cal}}^{\text{jet}}$. A total of 197 155 events with at least one jet satisfying $E_{T,\text{cal}}^{\text{jet}} > 13$ GeV and $-1 < \eta_{\text{cal}}^{\text{jet}} < 2.5$ were selected.

4. Monte Carlo simulation

The MC programs PYTHIA 6.1 [16] and HERWIG 5.9 [17] were used to generate resolved and di-

---

[53] The ZEUS coordinate system is a right-handed Cartesian system, with the Z axis pointing in the proton beam direction, referred to as the "forward direction", and the X axis pointing left towards the centre of HERA. The coordinate origin is at the nominal interaction point.

rect photoproduction events. In both generators, the partonic processes are simulated using leading-order matrix elements, with the inclusion of initial- and final-state parton showers. Fragmentation into hadrons was performed using the Lund string model [18] as implemented in JETSET [19] in the case of PYTHIA, and a cluster model [20] in the case of HERWIG. The generated events were used for calculating energy and acceptance corrections. The corrections provided by PYTHIA were used as default values and those given by HERWIG were used to estimate the systematic uncertainties coming from the treatment of the parton shower and hadronization. Samples of PYTHIA including multiparton interactions [21] with a minimum transverse momentum for the secondary scatter of 1 GeV [22] were used to study the effects of a possible "underlying event".

All generated events were passed through the ZEUS detector- and trigger-simulation programs based on GEANT 3.13 [23]. They were reconstructed and analyzed by the same program chain as the data. The jet search was performed using the energy measured in the CAL cells in the same way as for the data. The same jet algorithm was also applied to the final-state particles; the jets found in this way are referred to as hadronic jets.

5. Fixed-order QCD calculations

The QCD calculations, at both leading order (LO) and next-to-leading order (NLO), used in this analysis are based on the program by Klasen, Kleinwort and Kramer [24]. The calculations use the phase-space-slicing method [25] with an invariant-mass cut to isolate the singular regions of the phase space. The number of flavours was set to five; the renormalization, μ_R, and factorization scales, μ_F, were set to $\mu_R = \mu_F = \mu = E_T^{\text{jet}}$; α_s was calculated at two loops using $\Lambda_{\overline{\text{MS}}}^{(5)} = 220$ MeV, which corresponds to $\alpha_s(M_Z) = 0.1175$. The MRST99 [26] parameterizations of the parton distribution functions (PDFs) of the proton and the GRV [27] sets for the photon were used as defaults for the comparisons with the measured cross sections.

Since the measurements refer to jets of hadrons, whereas the QCD calculations refer to partons, the predictions were corrected to the hadron level using the MC models. The multiplicative correction factor, C_{had}, defined as the ratio of the cross section for jets of hadrons over that for jets of partons, was estimated with the PYTHIA and HERWIG programs. The values of C_{had} obtained with PYTHIA were taken as the defaults; the predictions from the two models were in good agreement. The values of C_{had} differed from unity by less than 2.5%.

6. Energy and acceptance corrections

The comparison of the reconstructed jet variables for the hadronic and the calorimetric jets in simulated events showed that no correction was needed for η^{jet} and φ^{jet} ($\eta^{\text{jet}} \simeq \eta_{\text{cal}}^{\text{jet}}$ and $\varphi^{\text{jet}} \simeq \varphi_{\text{cal}}^{\text{jet}}$). However, the transverse energy of the calorimetric jet was an underestimate of the corresponding hadronic jet energy by an average of $\sim 15\%$, with an r.m.s. of $\sim 10\%$. This underestimation was mainly due to the energy lost by the particles in the inactive material in front of the CAL. The transverse-energy corrections to calorimetric jets, as a function of $\eta_{\text{cal}}^{\text{jet}}$ and $E_{T,\text{cal}}^{\text{jet}}$ and averaged over $\varphi_{\text{cal}}^{\text{jet}}$, were determined using the MC events. Henceforth, jet variables without subscript refer to the corrected values. After these corrections to the jet transverse energy, events with at least one jet satisfying $E_T^{\text{jet}} > 17$ GeV and $-1 < \eta^{\text{jet}} < 2.5$ were retained.

The γp centre-of-mass energy is given by $W_{\gamma p} = \sqrt{sy}$, where y is the inelasticity variable and $\sqrt{s}$ is the ep centre-of-mass energy, $s = 4E_e E_p$. The inelasticity variable was reconstructed using the method of Jacquet–Blondel [28], $y_{\text{JB}} = (E - p_Z)/2E_e$, where E is the total CAL energy and p_Z is the Z component of the energy measured in the CAL cells. The value of y was systematically underestimated by $\sim 20\%$ with an r.m.s. of $\sim 10\%$. This effect, which was due to energy lost in the inactive material in front of the CAL and to particles lost in the rear beampipe, was satisfactorily reproduced by the MC simulation of the detector. The MC event samples were therefore used to correct for this underestimation [29] and obtain y_{cor}. Events were required to have $142 < W_{\gamma p} < 293$ GeV, where $W_{\gamma p} = \sqrt{s y_{\text{cor}}}$.

The variable x_T was reconstructed using the corrected values of E_T^{jet} and $W_{\gamma p}$. Its resolution was

$\sim 12\%$. The variable $\eta_{\gamma p}^{\text{jet}}$ was computed by boosting η^{jet} to the γp centre-of-mass frame using the formula $\eta_{\gamma p}^{\text{jet}} = \eta^{\text{jet}} - \ln(2E_p/W_{\gamma p})$. The comparison of $\eta_{\gamma p}^{\text{jet}}$ for the hadronic and the calorimetric jets in simulated events showed a good correlation, so that no correction was needed. The resolution on $\eta_{\gamma p}^{\text{jet}}$ was ~ 0.08.

The PYTHIA MC event samples of resolved and direct processes were used to compute the acceptance corrections to the jet distributions. These correction factors took into account the efficiency of the trigger, the selection criteria and the purity and efficiency of the jet reconstruction. The contributions from direct and resolved processes in the MC models were added according to a fit to the uncorrected data distribution of the energy deposited in the RCAL. A reasonable description of the E_T^{jet}, η^{jet}, $W_{\gamma p}$, $\eta_{\gamma p}^{\text{jet}}$ and x_T distributions in the data was provided by both PYTHIA and HERWIG. The differential inclusive jet cross sections were obtained by applying bin-by-bin corrections to the measured distributions. These correction factors differed from unity by typically less than 10%.

7. Experimental uncertainties

A detailed study of the experimental systematic uncertainties of the cross-section measurements included the following sources:

- The effect of the presence of a possible underlying event was estimated by using the samples of PYTHIA including multiparton interactions to evaluate the correction factors. This effect was typically 5% and increased to $\sim 10\%$ in the high-x_T tail of the scaled jet invariant cross sections;
- The effect of the treatment of the parton shower and hadronization was estimated by using the HERWIG generator to evaluate the correction factors. The uncertainty in the cross sections was typically 2%;
- The effect of the uncertainty on the modelling of the Q^2 spectrum of resolved processes in the MC was estimated by using the different approximations implemented in PYTHIA and HERWIG. The uncertainty in the cross sections was below 2%;

- The effect of the uncertainty on $W_{\gamma p}$ was estimated by varying y_{JB} by $\pm 1\%$ in simulated events. The uncertainty in the cross sections was below 1% at low E_T^{jet}, increasing to $\sim 3\%$ at high E_T^{jet};
- The effect of the uncertainty on the parameterizations of the proton and photon PDFs was estimated by using alternative sets of PDFs in the MC simulation to calculate the correction factors. The variation of the cross sections was smaller than 1% in each case.

The uncertainty on the simulation of the trigger was negligible. All the above systematic uncertainties were added in quadrature, giving a total systematic uncertainty in the cross sections of 5% at low E_T^{jet}, increasing to $\sim 10\%$ at high E_T^{jet}. The absolute energy scale of the calorimetric jets in simulated events was varied by its uncertainty of $\pm 1\%$ [10,30]. The effect of this variation on the inclusive jet cross sections was typically $\mp 5\%$ at low E_T^{jet} increasing to $\mp 10\%$ at high E_T^{jet}. This uncertainty is highly correlated between measurements in different bins. The uncertainty in the luminosity determination of 2.25% was not included.

8. Uncertainties on the theoretical predictions

The following uncertainties were considered:

- The uncertainty on the NLO calculations due to higher-order terms was estimated by varying μ between $E_T^{\text{jet}}/2$ and $2E_T^{\text{jet}}$. It was less than 10% and mainly affected the normalization. In the ratio of the scaled jet invariant cross sections, it was less than 2.5%;
- The uncertainty on the NLO calculations due to the uncertainties on the photon PDFs was estimated by using an alternative set of parameterizations, AFG-HO [31]. The effect was below 5% for the cross sections and 2% for the ratio;
- The uncertainty on the NLO calculations due to the statistical and correlated systematic experimental uncertainties of each data set used in the determination of the proton PDFs was calculated, making use of the results of an analysis [32] that

provided the covariance matrix of the fitted PDF parameters and the derivatives as a function of Bjorken x and μ_F^2. The resulting uncertainty in the cross sections was 1% at low E_T^{jet} and increased to 5% at high E_T^{jet}. The uncertainty in the ratio of the scaled jet invariant cross sections was below 0.3%. To estimate the uncertainties on the cross sections due to the theoretical uncertainties affecting the extraction of the proton PDFs, the calculation of all the differential cross sections was repeated using a number of different parameterizations obtained under different theoretical assumptions in the DGLAP fit [32]. This uncertainty was below 3% for the cross sections and negligible for the ratio;

- The uncertainty on the NLO calculations due to that on $\alpha_s(M_Z)$ was estimated by varying $\alpha_s(M_Z)$ within its uncertainty [33] and, simultaneously, by repeating the calculations using two additional sets of proton PDFs, MRST99↑↑ and MRST99↓↓, determined assuming $\alpha_s(M_Z) = 0.1225$ and 0.1125, respectively. The difference between the calculations using these sets and MRST99 was scaled by 60% to reflect the current uncertainty on the world average of α_s [33]. The resulting uncertainty in the cross sections was $\sim 8\%$ at low E_T^{jet} decreasing to $\sim 2\%$ at high E_T^{jet}. The uncertainty in the ratio of the scaled jet invariant cross sections was below 4%;

- The difference in the hadronization corrections as predicted by PYTHIA and HERWIG resulted in an uncertainty smaller than 2.5%.

All the above theoretical uncertainties were added in quadrature.

9. Results

9.1. Inclusive jet differential cross sections

Using the selected data, inclusive jet differential cross sections were measured for $142 < W_{\gamma p} < 293$ GeV. The cross sections were determined for jets with $E_T^{\text{jet}} > 17$ GeV and $-1 < \eta^{\text{jet}} < 2.5$. There were $113\,843$ events, containing $145\,797$ jets, in this kinematic region.

The cross-section $d\sigma/dE_T^{\text{jet}}$, measured in the E_T^{jet} range between 17 and 95 GeV, is presented in Fig. 1. The data points are located at the weighted mean of each E_T^{jet} bin. The measured $d\sigma/dE_T^{\text{jet}}$ falls by over five orders of magnitude in this E_T^{jet} range. Fig. 2 shows the scaled jet invariant cross section,

$$\left(E_T^{\text{jet}}\right)^4 \left\langle \frac{E^{\text{jet}} d^3\sigma}{dp_X^{\text{jet}} dp_Y^{\text{jet}} dp_Z^{\text{jet}}} \right\rangle_\eta,$$

averaged over the range $-2 < \eta_{\gamma p}^{\text{jet}} < 0$, as a function of x_T for $\langle W_{\gamma p} \rangle$ values of 180 and 255 GeV; the $\langle W_{\gamma p} \rangle$ values were chosen as the centres of the intervals 169–191 GeV and 240–270 GeV. The measurements were restricted to the same range in $\eta_{\gamma p}^{\text{jet}}$ to have the same acceptance for the two $\langle W_{\gamma p} \rangle$ intervals.

Fixed-order QCD calculations are compared to the data in Fig. 1. The LO QCD calculation underestimates the measured cross section by about 50% for $E_T^{\text{jet}} < 45$ GeV. The calculation that includes NLO corrections gives a good description of the data within the experimental and theoretical uncertainties over the complete E_T^{jet} range studied. In particular, no significant deviation is observed in the highest E_T^{jet} region. The NLO calculations also give a good description of the scaled jet invariant cross sections as a function of x_T, as shown in Fig. 2.

9.2. Test of scaling

To test the scaling hypothesis, the ratio of the scaled jet invariant cross sections as a function of x_T was measured for the two chosen values of $\langle W_{\gamma p} \rangle$, after correcting for the difference in the photon flux [34] between these intervals. Fig. 3 shows the measured ratio as a function of x_T. It shows a clear deviation from unity, in agreement with the NLO QCD predictions, which include the running of α_s and the evolution of the PDFs with the scale. The evolution causes the predicted ratio to change non-monotonically with x_T. The deviation from unity constitutes the first observation of scaling violations in γp interactions.

The ratio of the scaled jet invariant cross sections can be used to test QCD more precisely than is possible with the individual cross sections, since the experimental and theoretical uncertainties partially cancel. In particular, the experimental uncertainty in
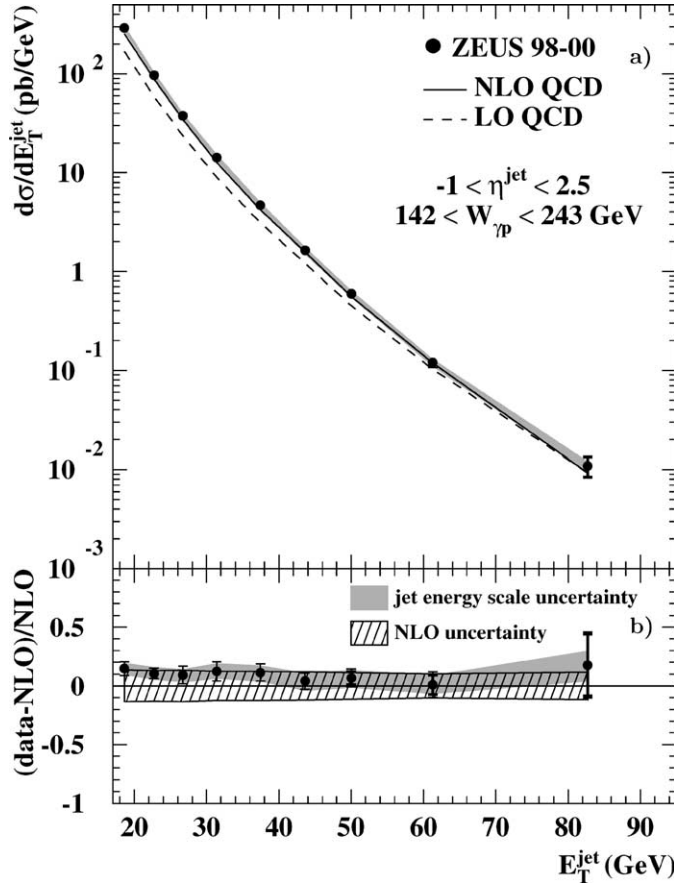
Fig. 1. (a) Measured inclusive jet cross section, $d\sigma/dE_T^{\text{jet}}$ (dots). The thick error bars represent the statistical uncertainties of the data, and the thin bars show the statistical and systematic uncertainties added in quadrature. The uncertainty associated with the absolute energy scale of the jets is shown separately as a shaded band. The LO (dashed line) and NLO (solid line) QCD parton-level calculations corrected for hadronization effects are also shown. (b) The fractional difference between the measured $d\sigma/dE_T^{\text{jet}}$ and the NLO QCD calculation; the hatched band shows the uncertainty of the calculation.

the absolute energy scale of the jets cancels almost completely in the ratio. The theoretical uncertainty on the predictions of the scaled jet invariant cross section was 13%, whereas that on the ratio was reduced to 2–5%. The NLO QCD prediction is in agreement with the data within the improved experimental (below 12%) and theoretical uncertainties. This agreement shows that the energy-scale dependence predicted by QCD is in accord with the measured dependence.

9.3. Determination of $\alpha_s(M_Z)$

The measured cross-section $d\sigma/dE_T^{\text{jet}}$ as a function of E_T^{jet} was used to determine $\alpha_s(M_Z)$ us-

ing the method presented previously [35]. The NLO QCD calculations were performed using the three MRST99 sets of proton PDFs, central, MRST99↓↓ and MRST99↑↑; the value of $\alpha_s(M_Z)$ used in each partonic cross-section calculation was that associated with the corresponding set of PDFs. The $\alpha_s(M_Z)$ dependence of the predicted $d\sigma/dE_T^{\text{jet}}$ in each bin i of E_T^{jet} was parameterized according to

$$\left[\frac{d\sigma}{dE_T^{\text{jet}}(\alpha_s(M_Z))} \right]_i = C_1^i \alpha_s(M_Z) + C_2^i \alpha_s^2(M_Z),$$

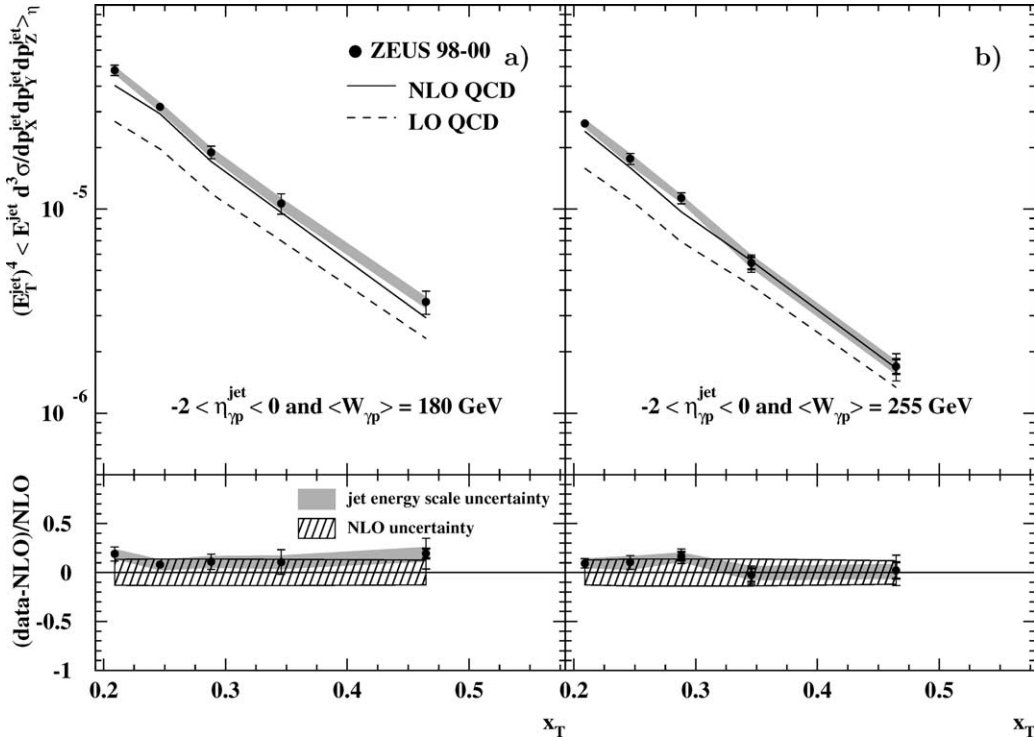where C_1^i and C_2^i are constants, by using the NLO QCD calculations corrected for hadronization effects.

Fig. 2. Measured scaled jet invariant cross section, $(E_T^{\text{jet}})^4 \langle E^{\text{jet}} d^3\sigma/dp_X^{\text{jet}} dp_Y^{\text{jet}} dp_Z^{\text{jet}} \rangle_\eta$, averaged over $-2 < \eta_{\gamma p}^{\text{jet}} < 0$, as a function of x_T (dots) for (a) $\langle W_{\gamma p} \rangle = 180$ GeV, (b) $\langle W_{\gamma p} \rangle = 255$ GeV. Other details are as given in the caption to Fig. 1.

Finally, a value of $\alpha_s(M_Z)$ was determined in each bin of the measured cross section as well as from all the data points by a χ^2 fit.

The uncertainties on the extracted values of $\alpha_s(M_Z)$ due to the experimental systematic uncertainties were evaluated by repeating the analysis for each systematic check presented in Section 7. The largest contribution to the experimental uncertainty comes from the jet energy scale and amounts to $\pm 1.5\%$ on $\alpha_s(M_Z)$. The theoretical uncertainties were evaluated as described in Section 8. The largest contribution was the theoretical uncertainty on $\alpha_s(M_Z)$ arising from terms beyond NLO, which was $^{+4.2}_{-3.3}\%$. The change of $\alpha_s(M_Z)$ due to the uncertainties on the photon PDFs and on the hadronization corrections were $+0.7\%$ and $+0.8\%$, respectively. The uncertainty on $\alpha_s(M_Z)$ due to the uncertainties on the proton PDFs was $\pm 0.9\%$. The total theoretical uncertainty on $\alpha_s(M_Z)$ was obtained by adding these uncertainties in quadrature.

The values of $\alpha_s(M_Z)$ as determined from the measured $d\sigma/dE_T^{\text{jet}}$ in each region of E_T^{jet} are shown in

Fig. 4(a). By combining all the E_T^{jet} regions, the value of $\alpha_s(M_Z)$ obtained is

$$\alpha_s(M_Z) = 0.1224$$
$$\pm 0.0001 (\text{stat.})^{+0.0022}_{-0.0019}(\text{exp.})^{+0.0054}_{-0.0042}(\text{th.}).$$

This value of $\alpha_s(M_Z)$ is consistent with the current world average [33] of 0.1183 ± 0.0027 as well as with recent determinations from jet production in NC DIS at HERA [35,36] and $p\bar{p}$ collisions at Tevatron [37]. It has a precision comparable to the values obtained from e^+e^- interactions [33].

9.4. Energy-scale dependence of α_s

The QCD prediction for the energy-scale dependence of the strong coupling constant was explicitly tested by determining α_s from the measured $d\sigma/dE_T^{\text{jet}}$ at different E_T^{jet} values. The method employed was the same as described above, but parameterizing the α_s dependence of $d\sigma/dE_T^{\text{jet}}$ in terms of $\alpha_s(\langle E_T^{\text{jet}} \rangle)$ instead of
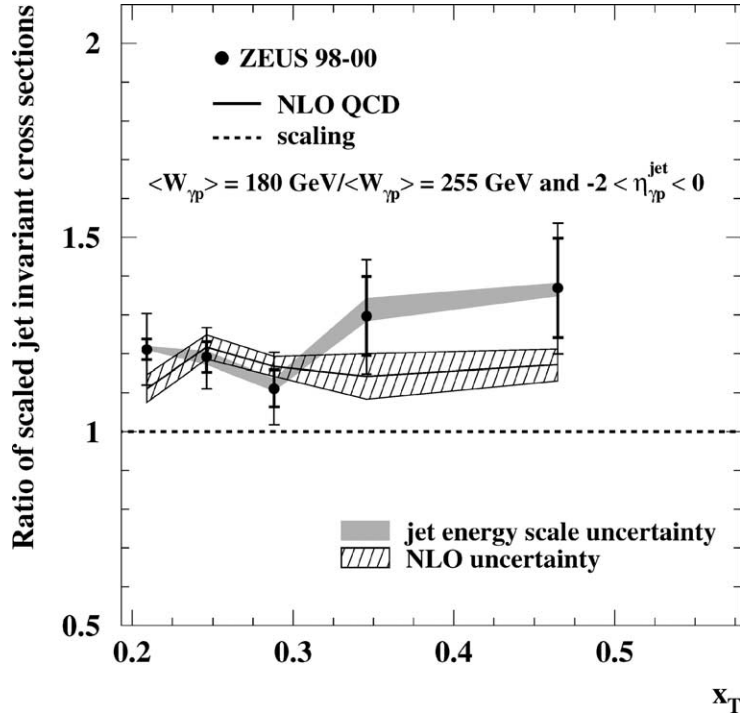
Fig. 3. Measured ratio of scaled jet invariant cross sections, after correcting for the difference in the photon flux between the two $W_{\gamma p}$ intervals, as a function of x_T (dots). The dashed line is the scaling expectation. Other details are as given in the caption to Fig. 1.

$\alpha_s(M_Z)$, where $\langle E_T^{\rm jet} \rangle$ is the weighted mean of $E_T^{\rm jet}$ in each bin. The measured $\alpha_s(E_T^{\rm jet})$ values are shown in Fig. 4(b). The results are in good agreement with the predicted running of the strong coupling constant over a large range in $E_T^{\rm jet}$.

The energy-scale dependence of the measured $\alpha_s(E_T^{\rm jet})$ was quantified by fitting the results using the functional form predicted by the renormalization group equation. Perturbative QCD predicts that $\alpha_s^{-1}(E_T^{\rm jet})$ varies approximately linearly with $\ln E_T^{\rm jet}$. At two loops, energy-scale dependence of $\alpha_s^{-1}(E_T^{\rm jet})$ is given by

$$\alpha_s^{-1}(E_T^{\rm jet}) = \frac{\beta_0}{2\pi} \ln(E_T^{\rm jet}/\Lambda)$$
$$\times \left[1 - \frac{\beta_1}{\beta_0^2} \frac{\ln(2\ln(E_T^{\rm jet}/\Lambda))}{\ln(E_T^{\rm jet}/\Lambda)} \right]^{-1}, \quad (1)$$

where $\beta_0 = 11 - \frac{2}{3}n_f$, $\beta_1 = 51 - \frac{19}{3}n_f$, and n_f is the number of active flavours. Thus, the slope of $\alpha_s^{-1}(E_T^{\rm jet})$ gives $\beta_0/2\pi$. A χ^2 fit to the extracted $\alpha_s^{-1}(E_T^{\rm jet})$ values

was performed to determine β_0 using the functional form given by Eq. (1), leaving β_0 and Λ as free parameters; β_1 was set to $(19\beta_0 - 107)/2$. Fig. 4(c) shows the measured $\alpha_s^{-1}(E_T^{\rm jet})$ as a function of $\ln E_T^{\rm jet}$ together with the results of the fit. Although the value of Λ, $0.535 \pm 0.073(\text{stat.})^{+0.140}_{-0.126}(\text{exp.})^{+0.506}_{-0.233}(\text{th.})$ GeV, is not well constrained in the fit, the value of $\alpha_s(M_Z)$ obtained by extrapolation from the results of the fit is more precise,

$$\alpha_s(M_Z) = 0.1188$$
$$\pm 0.0009(\text{stat.})^{+0.0043}_{-0.0039}(\text{exp.})^{+0.0069}_{-0.0067}(\text{th.}).$$

This determination of $\alpha_s(M_Z)$ is consistent with that of Section 9.3, in which the running of α_s as predicted by QCD was assumed. The extracted value of β_0 is

$$\beta_0 = 8.53 \pm 0.22(\text{stat.})^{+0.56}_{-0.53}(\text{exp.})^{+1.34}_{-0.82}(\text{th.}).$$

The correlation coefficient between β_0 and $\alpha_s(M_Z)$ is $\rho = -0.98$. This value is consistent with the prediction of perturbative QCD for the relevant number of active flavours in the $E_T^{\rm jet}$ region considered, $\beta_0 = 7.67$ for $n_f = 5$.
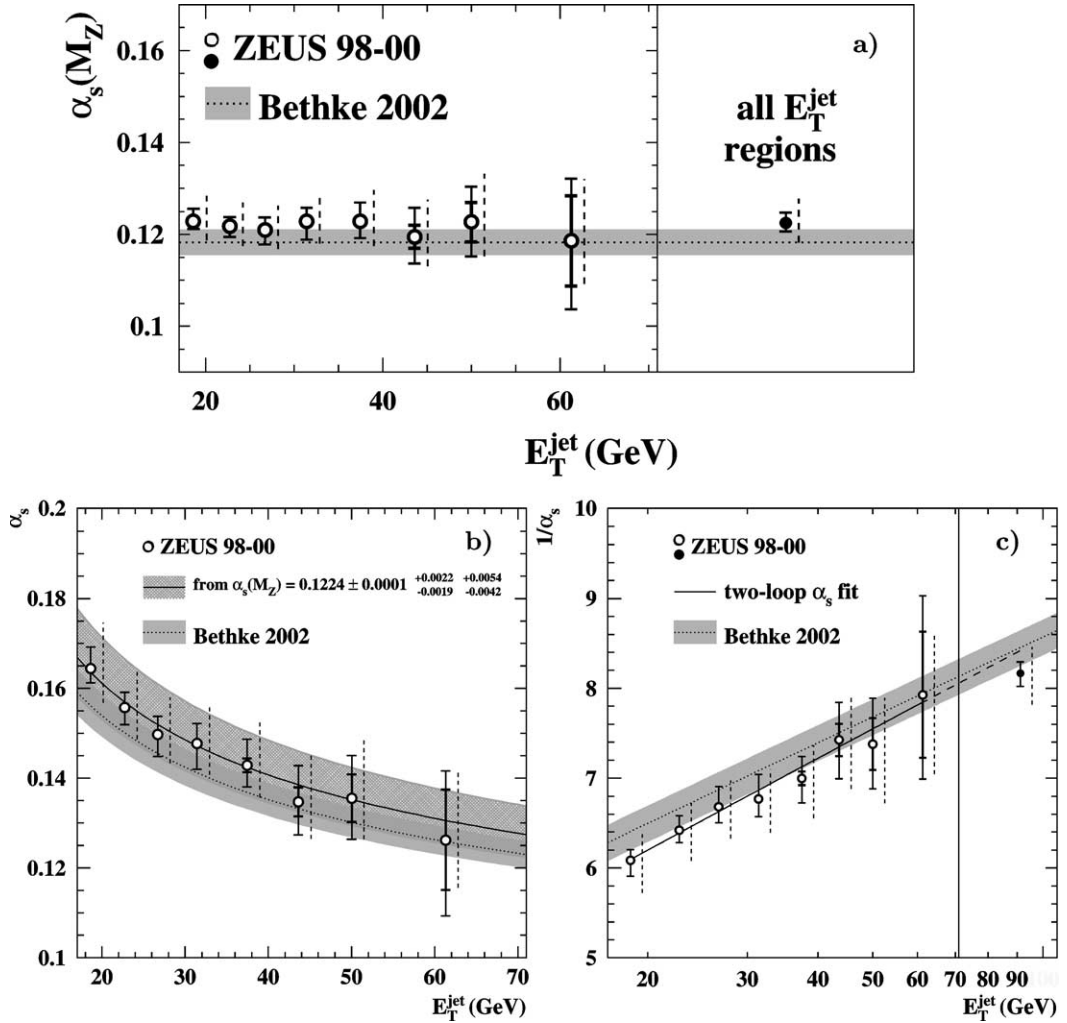
Fig. 4. (a) The $\alpha_s(M_Z)$ values determined from the QCD fit of the measured $d\sigma/dE_T^{\text{jet}}$ in the different E_T^{jet} regions (open circles). The combined value of $\alpha_s(M_Z)$ obtained using all the E_T^{jet} regions is shown as a dot. (b) The $\alpha_s(E_T^{\text{jet}})$ values determined from the QCD fit of the measured $d\sigma/dE_T^{\text{jet}}$ as a function of E_T^{jet} (open circles). The solid line represents the prediction of the renormalization group equation obtained from the $\alpha_s(M_Z)$ central value as determined in this analysis; the light-shaded area displays its uncertainty. (c) The $1/\alpha_s(E_T^{\text{jet}})$ values as a function of E_T^{jet} (open circles). The solid line represents the result of the two-loop α_s fit to the measured values. The dashed line represents the extrapolation of the result of the fit to $E_T^{\text{jet}} = M_Z$. The dot, plotted at $E_T^{\text{jet}} = M_Z$, represents the inverse of the combined value shown in (a). In all figures, the inner error bars represent the statistical uncertainties of the data and the outer error bars show the statistical and systematic uncertainties added in quadrature. The dashed error bars represent the theoretical uncertainties. The current world average [33] (dotted line) and its uncertainty (shaded band) are displayed.

10. Summary and conclusions

Measurements of differential cross sections for inclusive jet photoproduction have been made in ep collisions at a centre-of-mass energy of 318 GeV using 82.2 pb^{-1} of data collected with the ZEUS detector at HERA. The cross sections refer to jets identified with the longitudinally invariant k_T cluster algorithm in the inclusive mode and selected with $E_T^{\text{jet}} > 17$ GeV and $-1 < \eta^{\text{jet}} < 2.5$. The measurements were made

in the kinematic region defined by $Q^2 \leqslant 1$ GeV^2 and $142 < W_{\gamma p} < 293$ GeV.

The inclusive jet cross section was measured as a function of E_T^{jet} in the range between 17 and 95 GeV. The scaled jet invariant cross sections, averaged over $-2 < \eta_{\gamma p}^{\mathrm{jet}} < 0$, were measured as a function of the dimensionless variable x_T for $\langle W_{\gamma p} \rangle = 180$ and 255 GeV. The NLO QCD calculations give a good description of the shape and magnitude of the measured cross sections. No significant deviation with respect to QCD was observed up to the highest scale studied. The ratio of scaled jet invariant cross sections at two values of $\langle W_{\gamma p} \rangle$ represents the first observation of scaling violations in γp interactions.

A QCD analysis of the measured $d\sigma/dE_T^{\mathrm{jet}}$ yields a value of the strong coupling constant of

$$\alpha_s(M_Z) = 0.1224$$

$$\pm\, 0.0001(\mathrm{stat.})^{+0.0022}_{-0.0019}(\mathrm{exp.})^{+0.0054}_{-0.0042}(\mathrm{th.}),$$

which is in agreement with the current world average and constitutes the first determination of $\alpha_s(M_Z)$ from jet production in γp interactions. The value of α_s as a function of E_T^{jet} is in good agreement, over a wide range of E_T^{jet}, with the running of α_s as predicted by QCD.

Acknowledgements

References

[1] CDF Collaboration, F. Abe, et al., Phys. Rev. Lett. 70 (1993) 1376;
DØ Collaboration, B. Abbott, et al., Phys. Rev. Lett. 86 (2001) 2523.

[2] C.H. Llewellyn Smith, Phys. Lett. B 79 (1978) 83;
I. Kang, C.H. Llewellyn Smith, Nucl. Phys. B 166 (1980) 413;
J.F. Owens, Phys. Rev. D 21 (1980) 54;
M. Fontannaz, A. Mantrach, D. Schiff, Z. Phys. C 6 (1980) 241.

[3] W.J. Stirling, Z. Kunszt, in: R.D. Peccei (Ed.), Proceedings of the HERA Workshop, Vol. 2, DESY, Hamburg, 1987, p. 331;
M. Drees, F. Halzen, Phys. Rev. Lett. 61 (1988) 275;
M. Drees, R.M. Godbole, Phys. Rev. Lett. 61 (1988) 682;
M. Drees, R.M. Godbole, Phys. Rev. D 39 (1989) 169;
H. Baer, J. Ohnemus, J.F. Owens, Z. Phys. C 42 (1989) 657;
H. Baer, J. Ohnemus, J.F. Owens, Phys. Rev. D 40 (1989) 2844.

[4] ZEUS Collaboration, M. Derrick, et al., Phys. Lett. B 293 (1992) 465.

[5] ZEUS Collaboration, U. Holm (Ed.), The ZEUS Detector, status report, (unpublished), DESY, 1993, available on http://www-zeus.desy.de/bluebook/bluebook.html.

[6] N. Harnew, et al., Nucl. Instrum. Methods A 279 (1989) 290;
B. Foster, et al., Nucl. Phys. (Proc. Suppl.) B 32 (1993) 181;
B. Foster, et al., Nucl. Instrum. Methods A 338 (1994) 254.

[7] M. Derrick, et al., Nucl. Instrum. Methods A 309 (1991) 77;
A. Andresen, et al., Nucl. Instrum. Methods A 309 (1991) 101;
A. Caldwell, et al., Nucl. Instrum. Methods A 321 (1992) 356;
A. Bernstein, et al., Nucl. Instrum. Methods A 336 (1993) 23.

[8] J. Andruszków, et al., preprint DESY-92-066, DESY, 1992;
ZEUS Collaboration, M. Derrick, et al., Z. Phys. C 63 (1994) 391;
J. Andruszków, et al., Acta Phys. Pol. B 32 (2001) 2025.

[9] W.H. Smith, K. Tokushuku, L.W. Wiggers, in: C. Verkerk, W. Wojcik (Eds.), Proceedings of the Computing in High-Energy Physics (CHEP), Annecy, France, September 1992, CERN, Geneva, Switzerland, 1992, p. 222, also in preprint DESY 92-150B.

[10] ZEUS Collaboration, S. Chekanov, et al., Phys. Lett. B 531 (2002) 9.

[11] H. Abramowicz, A. Caldwell, R. Sinkus, Nucl. Instrum. Methods A 365 (1995) 508;
R. Sinkus, T. Voss, Nucl. Instrum. Methods A 391 (1997) 360.

[12] ZEUS Collaboration, M. Derrick, et al., Phys. Lett. B 322 (1994) 287.

[13] S. Catani, et al., Nucl. Phys. B 406 (1993) 187.

[14] S.D. Ellis, D.E. Soper, Phys. Rev. D 48 (1993) 3160.

[15] J.E. Huth, et al., in: E.L. Berger (Ed.), Research Directions for the Decade, Proceedings of Summer Study on High Energy Physics, 1990, World Scientific, Singapore, 1992, p. 134, also in preprint FERMILAB-CONF-90-249-E.

[16] T. Sjöstrand, Comput. Phys. Commun. 82 (1994) 74.

[17] G. Marchesini, et al., Comput. Phys. Commun. 67 (1992) 465.

[18] B. Andersson, et al., Phys. Rep. 97 (1983) 31.

[19] T. Sjöstrand, Comput. Phys. Commun. 39 (1986) 347;

T. Sjöstrand, M. Bengtsson, Comput. Phys. Commun. 43 (1987) 367.

[20] B.R. Webber, Nucl. Phys. B 238 (1984) 492.

[21] T. Sjöstrand, M. van Zijl, Phys. Rev. D 36 (1987) 2019.

[22] ZEUS Collaboration, J. Breitweg, et al., Eur. Phys. J. C 2 (1998) 61.

[23] R. Brun, et al., GEANT3, technical report CERN-DD/EE/84-1, CERN, 1987.

[24] M. Klasen, T. Kleinwort, G. Kramer, Eur. Phys. J. Direct C 1 (1998) 1.

[25] G. Kramer, Theory of Jets in Electron–Positron Annihilation, Springer, Berlin, 1984.

[26] A.D. Martin, et al., Eur. Phys. J. C 4 (1998) 463; A.D. Martin, et al., Eur. Phys. J. C 14 (2000) 133.

[27] M. Glück, E. Reya, A. Vogt, Phys. Rev. D 45 (1992) 3986; M. Glück, E. Reya, A. Vogt, Phys. Rev. D 46 (1992) 1973.

[28] F. Jacquet, A. Blondel, in: U. Amaldi (Ed.), Proceedings of the Study for an *ep* Facility for Europe, DESY, Hamburg, Germany, 1979, p. 391, also in preprint DESY 79/48.

[29] ZEUS Collaboration, J. Breitweg, et al., Eur. Phys. J. C 4 (1998) 591.

[30] ZEUS Collaboration, S. Chekanov, et al., Eur. Phys. J. C 23 (2002) 615; M. Wing (on behalf of the ZEUS Collaboration), in: Proceedings of the 10th International Conference on Calorimetry in High Energy Physics, hep-ex/0206036.

[31] P. Aurenche, J.P. Guillet, M. Fontannaz, Z. Phys. C 64 (1994) 621.

[32] M. Botje, Eur. Phys. J. C 14 (2000) 285.

[33] S. Bethke, J. Phys. G 26 (2000) R27; Updated in: S. Bethke, hep-ex/0211012.

[34] S. Frixione, et al., Phys. Lett. B 319 (1993) 339.

[35] ZEUS Collaboration, J. Breitweg, et al., Phys. Lett. B 507 (2001) 70; ZEUS Collaboration, S. Chekanov, et al., Phys. Lett. B 547 (2002) 164.

[36] H1 Collaboration, C. Adloff, et al., Eur. Phys. J. C 19 (2001) 289.

[37] CDF Collaboration, T. Affolder, et al., Phys. Rev. Lett. 88 (2002) 042001.